Limnology and diatom ecology of shallow lakes in a rapidly thawing discontinuous permafrost peatland

Kristen A Coleman[a*], Grace N. Hoskin[a], Laura Chasmer[b], Joshua R. Thienpont[a], William L. Quinton[c] and Jennifer B. Korosi[a]

[a] *Faculty of Environmental and Urban Change, York University, Toronto, Ontario, Canada, M3J 1P3*

[b] *Department of Geography and Environment, University of Lethbridge, Lethbridge, Alberta, Canada, T1K 3M4*

[c] *Cold Region Research Centre, Wilfrid Laurier University, Waterloo, Canada, N2L 3C5*

*corresponding author: kcoleman@yorku.ca

This is an Accepted Manuscript of an article published by Taylor & Francis in the journal Inland Waters on February 1, 2023, available online: https://doi.org/10.1080/20442041.2022.2144699

Limnology and diatom ecology of shallow lakes in a rapidly thawing discontinuous permafrost peatland

Lakes in discontinuous permafrost peatlands are on the front lines of climate change, sensitive to even modest increases in air temperature. The aim of this study was to provide the first limnological characterization of shallow (~1-2 m depth) lakes in the Scotty Creek basin (Northwest Territories, Canada), a field site of circumpolar significance due to the existence of long-term ecohydrological monitoring going back decades. We use this as a foundation from which to advance our process-based understanding of the potential drivers of lake ecosystem change. Our results showed that dissolved organic carbon (DOC) and lake color were not correlated, a pattern that appears to be an important driver of diatom (siliceous single-celled algae) assemblages in these lakes. Diatoms in the study lakes tended to fall into one of two assemblage clusters. One cluster, comprised of small benthic Fragilariaceae and small *Navicula* species (*sensu lato)*, was found associated with higher lake color. The second cluster, comprised of *Encyonopsis* and large *Navicula* species, was found associated with high DOC, lower color, and the presence of a benthic moss mat. From this, we suggest that DOC quality is a primary control on lake ecology in this region for its role in controlling light penetration to the lake bottom. We hypothesized that the prevalence of nearshore fens and collapse scar wetlands would be important drivers of DOC, but this was not supported in the 9 study lakes for which we had available data to map shoreline features.

Keywords: high-resolution data, collapse scars, channel fens, climate change, lake browning, DOC

1. Introduction

Permafrost peatlands cover approximately 19% of the circumpolar permafrost region (Tarnocai et al. 2009) and contain globally significant stores of terrestrial carbon (Harris et al. 2021). Climate change and an accelerated rate of permafrost thaw have raised concerns about their future role in the global carbon cycle under a warming climate (Hugelius et al. 2020). Shallow lakes are abundant features across many permafrost peatland landscapes of the circumpolar North. They play a critical role in the cycling of water and chemical constituents across the landscape, and act as both sentinels and agents of environmental change. Consequently, attempts to decipher the future role of permafrost peatlands in the global carbon balance must include an understanding of how shallow lake ecosystem structure and function are likely to be altered with climate change (Cole et al. 2007).

Discontinuous permafrost landscapes are highly sensitive to even modest warming of air temperatures (Kettles and Tarnocai 1999; Spence et al. 2020). Models project that 40% of the world's permafrost could be lost by 2100 CE (SOCR 2021), with sporadic discontinuous permafrost regions potentially permafrost-free by mid-century (Chasmer and Hopkinson 2017). Permafrost thaw can manifest in several different ways: it can change the thickness of the seasonally thawed (i.e. active) layer, generate a layer of talik separating the underlying permafrost from the overlying active layer, and produce thermokarst terrain (Zhang et al. 1999; Zhang et al. 2005; Frey and McClelland, 2009). While changes in active layer thickness occur slowly (press disturbance), thermokarst development from the thawing of ice-rich permafrost manifests as a rapid (or pulse) disturbance (Vonk et al. 2015). In southern permafrost peatlands, wetland thermokarst processes typically predominate, which results in the conversion of forests into wetlands (Quinton et al. 2019).

Wetland thermokarst alters the hydrologic connectivity of the landscape by increasing the number, duration, and depth of flow paths (Smith 2007; Karlsson 2012; Quinton et al. 2019). The hydrological connectivity of a landscape in turn exerts a strong control over transportation of sediment, organic matter, and nutrients, with shallow lakes playing a critical role in the processing of these materials along hydrological cascades. Increased areal wetland coverage and hydrological connectivity, coupled with increased availability of terrestrial organic matter liberated from thawed soils, has the potential to increase the export of terrestrial organic carbon to lakes. As terrestrial organic carbon is typically highly colored, increased export of carbon from the catchment can result in a phenomenon known as lake browning (Wauthy et al. 2018). Lake browning alters light penetration, thermal regime, and oxygen dynamics in lakes, and can fuel heterotrophic energy pathways in lake food webs (Cole et al. 2006; Porcal et al. 2009; Vonk et al. 2015; Tanentzap et al. 2017).

Increases in lake DOC concentrations are predicted with continued permafrost thaw (Vonk et al. 2013; Wauthy et al. 2018), yet paleolimnological reconstructions of thermokarst lakes have provided mixed results regarding trajectories of lake DOC concentrations (Vonk et al. 2012; Bouchard et al. 2013; Thienpont et al. 2013; Coleman et al. 2015). This may be due, at least in part, to localized differences in catchment ecohydrological characteristics. Topography, permafrost extent, ground ice content, surficial geology, and Quaternary history have all been identified as key state factors that are likely to influence biogeochemical responses of watersheds to permafrost thaw (O'Neill et al. 2019, Vonk et al. 2019; Tank et al. 2020). Consequently, representation across broad geographic gradients is required to disentangle the trajectories and drivers of limnological change in northern lakes and make predictions at the circumpolar scale. Even within regions, responses of permafrost peatlands to warming can be variable, highlighting the need for a better understanding of the processes underlying ecosystem change (Sim et al. 2021). In this study, we contribute to addressing these knowledge gaps by providing the first limnological characterization of small, shallow lakes in the Scotty Creek basin of the southwestern Northwest Territories (Canada).

The Scotty Creek basin (61º180 N, 121º180 W) is a region of low-relief and extensive peatlands located at the northern extent of the sporadic discontinuous permafrost zone in the Taiga Plains Ecozone. Here, permafrost exists beneath treed peat plateaus, while surrounding wetlands, including channel fens and collapse scar wetlands (hereafter "collapse scars"), are predominately treeless and permafrost-free. Warming air temperatures, which has accelerated since ~1970, has resulted in the rapid loss of permafrost (Quinton et al. 2019). The region is predicted to be permafrost-free by mid-century (Chasmer and Hopkinson 2017). The Scotty Creek Research Station has supported intensive field, remote sensing, and modelling studies since the late ~1990's, providing a long-term perspective on thaw-induced watershed changes rarely available for remote subarctic regions (Quinton et al. 2019). To date, however, very little research has been done on the many small lakes and ponds found within the Scotty Creek basin. In a recent comparison of hydrological trends in 32 circumpolar peatland basins, the Taiga Plains was unique in experiencing a widespread increase in annual basin runoff in the absence of increasing precipitation (Mack et al. 2021), a phenomenon that has been linked to accelerated wetland thermokarst (Connon et al. 2012). Clearly, the Scotty Creek basin is in a period of rapid transition, where limnological research should be prioritized.

The objectives of this study are to: (1) document the present-day limnology of shallow lakes in the Scotty Creek basin as a benchmark from which to examine future limnological change; and (2) examine spatial relationships between water chemistry, nearshore landscape characteristics, and diatom (siliceous algae) assemblages to understand controls on limnological characteristics and make predictions about drivers of future change. To meet our objectives, we analyzed surface water chemistry and sedimentary diatom assemblages in 16 lakes in or near the Scotty Creek basin and used high-resolution aerial imagery available for 9 of the lakes to map channel fen and collapse scar area within 250 m of the lake perimeter. We also collected high-resolution logger data for depth, oxygen, light, and temperature profiles over the 2019 ice-free season in two lakes in the Scotty Creek basin that we propose as candidate sites for the establishment of a long-term lake monitoring program. Overall, this study provides a foundation for advancing our process-based understanding of the drivers of limnological change in rapidly thawing discontinuous permafrost peatlands.

2. Methods

2.1 Overview

We selected 16 lakes to sample for water chemistry and sedimentary diatom assemblages. The 16 lakes were chosen because they are in close proximity to one another, and centered on the Scotty Creek basin, which allowed us to explore the range of limnological variability within a small geographic area (Figure 1). Of the 16 lakes, 8 were located within the Scotty Creek basin, an additional 6 were located just outside the boundaries of the Scotty Creek watershed, and 2 (FS1 and FS2) were located northeast of Scotty Creek. FS1 and FS2 were slightly larger, and in a more fluvially-influenced catchment setting, compared to the other lakes.

For 9 of the 16 study lakes, including SC8 and the 8 lakes within the Scotty Creek basin, we were able to use previously available landscape classification data (Chasmer et al. 2014) to quantify the area within 250 m of the lake shoreline that was composed of fens and collapse scars. We used the landscape classification data to explore relationships between water chemistry, diatoms, and land cover. Two of the lakes within the Scotty Creek basin (First Lake and Goose Lake) are easily accessible from the Scotty Creek Field Station, which allowed us to conduct more intensive field sampling. For these lakes, we deployed loggers and collected water and sediments from adjacent wetlands to further refine our understanding of their limnology.

2.2 Field methods

The 16 lakes were sampled from the center of the lake by helicopter in mid-July, 2018 (Figure 1). That season, ice-off occurred between May 4 and 10, 2018. Conductivity and pH were measured at all sites *in situ* using a Hanna multiprobe, but oxygen measurements were not recorded due to equipment malfunction. Lake depths were measured using an acoustic depth sounder; however, depths were not used in statistical analyses because the interference of dense moss mats and macrophytes established on many lake bottoms prevented stabilized readings of the depth sounder. For many lakes, readings fluctuated by 10s of cm, which is significant for these shallow systems. For all sites, water samples were collected in two pre-sterilized 1-litre polyethylene bottles. One litre was filtered through 0.45 µm cellulose acetate filters within 24 hours of collection for analysis of dissolved organic carbon (DOC) and total dissolved nitrogen (TN). Unfiltered water was poured into 250 mL glass bottles containing 0.5 mL nitric acid, including a field blank using DI water, and sent to SGS Laboratories for elemental analysis (Montreal, QC, Canada). Sediment cores were collected from the 16 lakes using a Uwitec gravity corer with an internal diameter of 8.6 cm and sectioned into 0.5 cm intervals using a modified Glew (1988) extruder. The top 0.5 cm of each core was used for the analysis of modern diatom assemblages. Based on ^{210}Pb dating, the top 0.5 cm represented ~2-5 years of sediment accumulation in these lakes (Coleman and Korosi 2023).

In June 2019, surface water and sediments were sampled from Goose Lake and First Lake at the Scotty Creek Research Station, as well as five fen sites and one collapse scar site (Figure 1D). Additionally, substrate samples (submerged vegetation, submerged peat, sediment, and grasses) were collected from shoreline environments around Goose Lake, and from a benthic moss mat in the centre of the north basin of Goose Lake at a water depth of ~1m. Water and sediment sampling followed the same methods used for the 2018 sampling of the 16 lakes, described above, except this time we were able to collect to collect dissolved oxygen data with the Hanna Multiprobe

Buoys equipped with HOBO Pendant wireless temperature and light data loggers, Onset HOBO U26 dissolved oxygen (DO) data loggers and Onset HOBO U20 depth loggers were deployed in both the main basin and northern basin of Goose Lake and center of First Lake (Figure 1D) on June 7th (~a month past ice-off) and removed on August 22nd, 2019. Each buoy was connected to a rope which was anchored to the sediment using 20 lb weights. An additional rope was suspended from the buoy, upon which three temperature/light loggers, and one oxygen logger were attached. The depth logger was attached to the weight to keep it stationary in the water column in relation to the sediments and was kept afloat using empty 2 L bottles. Precipitation data was collected using a Pluvio totalizing station, located at the Scotty Creek research station adjacent to Goose Lake, and was corrected for undercatch. Precipitation was recorded every 30 minutes to examine the impact of precipitation on other time-series data (e.g. light and depth).

2.3 Laboratory analysis of water chemistry

DOC and TN were analyzed on a Shimadzu-TOC5000 Series TOC-L analyzer following the combustion catalytic oxidation method and non-dispersive infrared detection. Standards were made using potassium hydrogen phthalate for instrument calibration and performance. Samples were acidified using HCl and sparged to purge DIC. True color was measured using the platinum-cobalt method on a Genesys 10S UV-Vis spectrophotometer (APHA 2011). Alkalinity was analyzed by titrating samples with 0.02N H_2SO_4 (APHA 1998). Samples were sent to SGS Laboratories (Montreal, QC, Canada) for elemental analysis, including total phosphorus, using ICP-MS and ICP-OES. Although perchloric acid digestion followed by colorimetry is the more common for analysis of total phosphorus, good agreement has been found between this method and ICP-MS (Ivanov et al., 2012), as used here.

2.4 Physical Landscape Characterization

2.3.1 Shoreline Development and Lake Area

The shoreline development (D_L) ratio, an index that describes how close a lake is to a perfect circle, was calculated for all 16 study lakes. Lakes with a D_L close to 1 have circular shapes, while lakes with high D_L have more jagged and crenulated shapes. D_L is the ratio of the perimeter of the lake to the perimeter of a circle with the same area

$$D_L = S_L \div 2 \cdot \mathrm{sqrt}(\pi \cdot A_o) \quad (1)$$

where S_L is shoreline length, and A_o is the area of the lake. Lakes with a higher D_L have higher potential for the development of littoral communities and increase the exposure of lakes to the surrounding shorelines. Lake area and perimeter were calculated using the polygon function in Google Earth.

2.3.2 *Buffer and Overlay Landscape Analysis*

Nine of the 16 study lakes were used for the buffer and overlay landscape analysis. Buffering is the process of creating an output polygon layer that delineates a zone of specified width around a feature of interest. An overlay is the process of taking two or more different maps of the same area and placing them on top of one another. In this study, we applied a 250 m buffer around the perimeter of the 9 study lakes, followed by an overlay analysis to determine how much fen and collapse scar area fell within each buffer. The outputted layers included shapefiles only of the collapse scars and fens that overlapped within the 250 m buffer. The buffer and overlay analyses were done in ArcMap version 10.7.1 using a raster file of the Scotty Creek study area. Individual shapefiles were created for each land classification (channel fen, collapse scars, water, moraine/upland, and permafrost) and the water layer was separated into individual lakes.

2.5 Subfossil Diatom Analysis

Diatom slides were prepared following Battarbee et al. (2001) using the hydrogen peroxide method and mounted using Naphrax®. Diatom valves were identified using an Amscope B690C-PL microscope and multiple reference texts (Krammer and Lange-Bertalot 1997; Krammer and Lange-Bertalot 1999; Krammer and Lange-Bertalot 2000; Fallu et al. 2000) and online databases (Guiry and Guiry, 2021; Spaulding et al. 2022). Between 300 to 500 valves were counted per site, except for Fen 4 and the collapse scar site which had markedly low diversity (Hill's N2 <4), where a minimum of 175 valves were counted. Diatom species were grouped based on similar ecologies (Appendix A) and were displayed as relative abundances. Chrysophyte cysts, which can form in response to changing environmental conditions, and protozoan plates, which can provide information on moisture levels, were also present on diatom slides and enumerated and displayed on figures as percentages relative to the sum of all diatom valves.

2.6 Data Analysis

Data retrieved from data loggers was plotted using the ggplot package (Wickham 2019) in R (R Core Team 2020). Light absorption per cm was calculated by the equation

$$[100 \text{ x } (I_0 - I_z)]/I_0 \qquad (2)$$

where I_0 is the irradiance recorded in the shallowest sensor, and I_z is the irradiance recorded in the deepest sensor divided by the number of cm between the two sensors. Anomalous negative values caused by higher irradiance values recorded in the deeper sensor than the shallower sensor were removed, and likely are a result of shading of the shallower sensor by the buoy. A LOESS smoothed line was included in the figures using the stat_smooth function in ggplot in R.

Water chemistry variables that had concentrations below detection were not included in any statistical analyses (mercury, silver, arsenic, beryllium, boron, bismuth, molybdenum, nickel, antimony, selenium, tin, thallium, zirconium, and zinc). Variables were also removed if there was evidence of contamination based on anomalously high field blank concentrations (aluminum, cadmium, cobalt, chromium, copper, iron, lead, titanium, uranium, and vanadium). Spearman's correlation analyses, used here due to the non-normal distribution of most variables, were calculated on remaining water chemistry variables to determine if there were statistically significant relationships between water chemistry variables and lake area (Area) or shoreline development (D_L). Water chemistry variables included in the Spearman's correlation analyses included pH, dissolved organic carbon (DOC), total nitrogen, filtered (TN), true color (color), phosphorus (TP), conductivity, alkalinity, calcium (Ca), potassium (K), lithium (Li), magnesium (Mg), manganese (Mn), sodium (Na), silicon (Si), and strontium (Sr).

Principal components analysis (PCA) was used to visualize limnological variation among lakes. Variables were standardized using the "scale" function in the vegan package (Oksanen et al. 2019) in R. A PCA was generated for all 16 lakes to examine variation between lakes with respect to Area, D_L, pH, DOC, TN, color, conductivity, Li, and Mn. Area and D_L were plotted passively. Highly correlated variables were removed from the PCA. For example, conductivity was correlated with alkalinity, calcium (Ca), potassium (K), magnesium (Mg), and strontium (Sr). The remaining variables were selected due to their importance in structuring biological communities (pH, DOC, TN, TP, color, and conductivity), usefulness as a lithogenic tracer (Li), or sensitivity to redox conditions (Mn). Li, TP, and Area were normalized using a log transformation, and D_L and conductivity were normalized using a loglog transformation. The remaining variables were already normally distributed, and no transformation was applied. A PCA was also generated for the subset of 9 lakes used in landscape analyses, to visually examine relationships between the same water chemistry variables as above and collapse scar or fen coverage within 250 m of the lake perimeter. Collapse scar and fen coverage were plotted passively, and Mn was normalized using a log transformation.

Direct ordination [Redundancy analysis (RDA)] was used to evaluate relationships between diatom community composition and environmental variables. Lake area and conductivity were log transformed to normalize distribution, and species data were Hellinger transformed to standardize species assemblage data from absolute to relative values. A variance inflation factor (VIF) test was run to assess multicollinearity. Variables with high VIFs were sequentially removed from analysis until all environmental variables had VIFs below 10.

Variables retained in the analysis were pH, color, DOC, area, and conductivity. Significance of the RDA was determined using an ANOVA-like permutations test. Correlation analyses were conducted using the Hmisc package (Harrell 2021), and PCAs, VIFs, RDAs and permutation tests were conducted using the Vegan package (Oksanen et al. 2019) in R.

3. Results

3.1 High-Resolution Assessment of Goose Lake and First Lake

Depth measurements obtained from depth loggers deployed in First Lake and the two main basins of Goose Lake (Figure 1D) from June 7th to August 22nd showed good agreement between all three loggers and suggested water levels of these shallow (~1 m) lakes fluctuated by ~30-40 cm throughout this period (Figures 2A, 2B, and 2C). Water levels fluctuated through June and July and began to stabilize towards the end of the recorded period. Lowest water levels occurred in early to mid-June and mid-July. Bottom dissolved oxygen (DO) measurements ranged from 5 to 12.5 mg/L in Goose Lake, in both the north basin (Figure 2A), and the main basin (Figure 2B). In First Lake, DO measurements appeared to have dropped to 0 mg/L for periods of time, however this was likely a result of the logger dropping into the sediments, as the logger recorded these anoxic conditions during periods of lower water levels (Figure 2C).

The consistency between temperature readings at different depths indicated that the entire water column in both lakes was mixed throughout the recorded period (Figure 2). Temperature measurements were consistent between lakes and fluctuated between 10 and 25^{o}C throughout the recorded period. All lakes recorded warmer periods in mid-June and late July/early August. The calculated % absorption of light per cm was similar between Goose Lake and First Lake, and although light penetration fluctuated through time, no clear seasonal trends were apparent (Figure 2); however, in Goose Lake, periods of higher light absorption (e.g. in late July) coincided with warmer temperatures (Figures 2A and 2B). Rainfall events occurred sporadically throughout the season, with the largest rainfall event occurring on July 18th when 12.4 mm of rain fell over an hour. Lake depth increased by ~20 cm in Goose Lake and First Lake after this rainfall event, and maximum depth occurred on July 23rd (Figure 2).

3.2 Characterization of lakes in or near the Scotty Creek Basin

3.2.1 Morphology and water chemistry of the 16 lakes

In 2018, lake depths of the 16 surveyed lakes ranged from ~0.9 to 2.1 m; however, dense macrophyte stands or benthic moss mats likely interfered with sonar measurements, as measurement readings in some lakes did not stabilize and fluctuated by tens of centimetres. Lake area ranged from 11 to 244 ha, except for a notably larger lake (FS1) that had an area of 713 ha (Table 1). Lakes were circumneutral to slightly alkaline (pH = 7.85 – 8.75). Alkalinity ranged from 28-124 mg/L $CaCO_3$, conductivity ranged from 55.5 to 244.2 µS/cm, DOC ranged from 12.96 to 23.74 mg/L, and water color ranged from 18-463 TCU (Table 1). TN (filtered) ranged from 0.54 to 1.54 mg/L, and TP (unfiltered) ranged from 8 to 38 µg/L.

3.2.2 Near-shore landscape characterization of 9 selected thermokarst lakes

Landscape coverage of fen environments varied between 0 and 34% within 250 m of the perimeters of the 9 lakes included in the landscape characterization analyses. Collapse scars were more extensive, covering between 13.4 and 48.9% of the landscape within 250 m of the lake perimeters (Figure 3). Lakes were generally well connected through channel fen networks, except for SC5 and SC8 that were more isolated. SC8 had no fen environment within 250 m of the lake, indicating it may be hydrologically isolated, and while SC5 had a fen-like environment containing grasses and sedges along the western edge of its shoreline, this fen was not hydrologically connected to a channel fen network (Figure 3).

3.2.3 Water chemistry of wetland environments near Goose and First Lake

The five fen environments had lower pH ranges than sampled lakes, being circumneutral to slightly acidic (5.97-7.40), and had higher DOC concentrations than lakes ranging from 23.08 to 33.7 mg/L. In comparison to this study, Gordon et al. (2016) previously reported lower pH values (5.15-5.46), and higher DOC values (~42-49 mg/L) for fens in the Scotty Creek basin. Water color ranged from 54 to 459 TCU, alkalinity ranged from 26 to 50 mg/L $CaCO_3$, TN ranged from 0.52 to 0.91 mg/L, and conductivity ranged from 25 to 82 μS/cm. DO ranged from 2.06 to 9.27 mg/L (or 17.6 to 89.7% saturation), and was slightly lower than what had been recorded by data loggers in Goose Lake and First Lake. The one collapse scar sampled had high DOC (46.8 mg/L), which was in range of values reported by Gordon et al. (2016), and also had high color (522 TCU), low pH (5.33), low alkalinity (4 mg/L $CaCO_3$) and low conductivity (25 μS/cm). TN (0.59 mg/L) and DO (6.35 mg/L; 58.5% saturation) was within the range of water chemistry variables measured in the 5 fen environments.

3.2.4 Analysis of relationships between water chemistry and landscape features

Principal components analysis (PCA) axis 1 explained 50% of the variation in water chemistry in the 16-lake dataset, largely driven by conductivity, lithium (Li), manganese (Mn), total nitrogen (TN), and color, while PCA axis 2 explained 23% of the variation in the data set and was largely driven by DOC and TP (Figure 4A). Generally, lakes were well dispersed throughout the ordination space; however, SC3, SC8, SC1, SC2, Next Lake, SC4, SC9, SC11 were well dispersed along PCA axis 2, but not axis 1, indicating these lakes differed in water chemistry variables associated with axis 2 (DOC and TP). Some lakes appeared to have similar water chemistry (e.g. SC2 and Next Lake; Figure 4A), despite being relatively far apart in physical space (Figure 1). PCA ordination of the 9-lake dataset (Figure 4B) illustrated the relationship between the same water chemistry variables examined in Figure 4A and proportion of collapse scar and fen environments within 250 m of lakes. Here, PCA axis 1 explained 46% of the variation in the dataset and was driven by conductivity, Mn, TN, Li, and TP, while PCA axis 2 explained 21% of the dataset and was driven by pH, color, and DOC (Figure 4B).

Correlation analyses suggested that lake area in this region was strongly ($r>0.6$) and positively correlated to conductivity, ($r=0.79$, $p<0.01$), alkalinity ($r=0.85$, $p<0.01$), major ions such as Ca ($r=0.74$, $p<0.01$), Mg ($r=0.77$, $p<0.01$) , and K ($r=0.78$, $p<0.01$) and moderately ($0.3>r<0.6$) and positively correlated with TN ($r=0.54$, $p<0.05$), Mn ($r=0.53$, $p<0.05$), and Sr ($r=0.57$, $p<0.05$)(Table 6). Lake area was also found to be strongly and negatively correlated to color ($r = -0.85$, $p<0.01$) (Table 2). Shoreline development index was moderately and positively correlated with conductivity ($r=0.50$, $p<0.05$) and Mg ($r=0.48$, $p<0.05$) (Table 2). DOC was moderately and positively correlated to both TN ($r=0.52$, $p<0.05$) and TP ($r=0.58$, $p<0.05$) (Table 2). TN was not significantly correlated to TP ($r=0.48$, $p>0.05$) (Table 2). Color was moderately, and negatively correlated to pH ($r=-0.54$, $p<0.05$), and strongly and negatively related to TN ($r=0.69$, $p<0.01$), while TN was moderately and positively related to lithium ($r=0.50$, $p<0.05$) (Table 2). DOC and color were not correlated in these lakes ($r=0.16$, $p=0.55$) (Table 2).

3.3 Diatom communities

3.3.1 Lakes

With a few exceptions, two common diatom assemblages were identified in the small lakes within the Scotty Creek basin and surrounding areas. The first assemblage, identified in SC9, SC3, SC2, SC1, SC5, and SC11, was dominated by small benthic Fragilariaceae (mainly *Pseudostaurosira brevistriata*, *P. parasitica*, *Staurosira construens*, and *S. venter)* and small *Navicula* species *sensu lato*, including *Sellaphora nigri*, and *Sellaphora seminulum* (Figure 5). The second assemblage, identified in SC4, SC6, SC12, Next Lake, FS2, Goose Lake, and SC10 was dominated by *Encyonopsis* species (*E. cesatii* and *E. descripta*), and large *Navicula* species (*N. cryptocephala*, *N. cryptotenella*, and *N. radiosa*). Many of these lakes (SC12, Goose Lake, SC10, Next Lake, and FS2) also had high abundances of *Brachysira* species (*B. styriaca*, *B. vitrea*, and *B. zellensis*) (Figure 5). There were a few exceptions to these common groupings: The assemblage in FS1 was dominated by *Achnanthidium minutissimum*; the assemblage in SC8 was dominated by *Achnanthidium minutissimum,* large *Navicula* species, *Nitzschia* species*, and Brachysira* species; and the assemblage in First Lake was dominated by *Achnanthidium minutissimum*, large *Navicula* species, *Nitzschia* species (mainly *N. fonticola* and *N. palea*), and centric planktonic species (*Lindavia michiganiana*, and *Discostella pseudostelligera*) (Figure 5). The abundance of chrysophyte cysts relative to diatom valves was variable, ranging from 0 to ~20%. Higher abundances were found in SC3 (~20%) and SC11 (~19%) and absent in FS1 and SC9. Protozoan plates were present in low abundance in most lakes (~0.2-4.6%) and absent in SC9 and SC10 (Figure 5).

Redundancy analysis (RDA) of diatom assemblages and pH, color, dissolved organic carbon, lake area, and conductivity was statistically significant ($F=1.8422$, $p<0.05$). The selected variables collectively explained 47.9% of the variance in the diatom assemblages, 40% of which was explained in the first two RDA axes (Figure 6). Some species preferences were identified in the RDA. For example, *Brachysira vitrea* was found to be associated with lakes with greater surface area*. Navicula cryptocephala. N. radiosa, Encyonopsis cesatii, E.descripta, Kobayasiella jaagi, Cymbopleura incerta*, and *Brachysira styriaca* were all found to be associated with lakes with higher DOC, while *Staurosira construens, Staurosira venter* , and *Pseudostaurosira brevistriata* were associated with high color. Lakes SC1, SC2, SC3, SC5, and SC9 had a similar diatom assemblage, while Next Lake, Goose Lake, and lakes SC4, SC6, SC10 and SC12 had similar assemblages. FS2, SC8, and First Lake also had a similar assemblage (Figure 6).

3.3.2 Wetland diatom assemblages

Diatom assemblages identified in the wetland samples were variable but exhibit notable differences from lake diatom assemblages. The most abundant diatoms found in fen environments were *Eunotia* species (mainly *E. bilunaris* and *E. subarcuatoides*), *Gomphonema* species (mainly *G. parvulum*), and *Tabellaria* spp. *Rossithidium pusillum, Achnanthidium minutissimum* (Figure 7)*, Nitzschia* species (mainly *N. fonticola* and *N. palea*), large *Navicula* species (mainly *N. cryptocephala*, *N. cryptotenella*, and *N. radiosa)*, *Kobayasiella subtilissima,* and planktonic *Fragilaria* (mainly F. *tenera*) species were also present (Figure 7). The relative abundances of chrysophyte cysts (7-36%) and protozoan plates were variable (2-37%), but generally higher in fens than lakes (Figure 7). The diatom assemblage in the collapse scar sample was dominated by *Kobayasiella subtilissima* (95%). The highest relative abundances of both chrysophyte cysts and protozoan plates were found in the collapse scar sample (both at 42% relative abundance) (Figure 7)

3.3.3 Diatom assemblages identified in lake substrate samples

In the lake substrate samples, *Tabellaria* spp and large *Navicula* species (mainly *N. cryptocephala*, *N. cryptotenella*, and *N. radiosa)* were the most abundant diatom species identified. *Tabellaria* spp was present in high abundances in grass (~48%) and submerged vegetation (~71%) samples and was also present in the submerged peat sample (~11%) (Table 3). Large *Navicula* species were found in high abundance in the sediment (~38%), submerged peat (~30%) and benthic moss mat (~39%) samples (Table 3). In addition to the large *Navicula* species, the diatom assemblage identified in the sediment sample also consisted of planktonic *Fragilaria* species (mostly *F. tenera*), *Encyonema* species (mostly *E. silesiacum*) and *Brachysira* species (*B. styriaca and B. vitrea*) (Table 3). The submerged peat sample also contained planktonic *Fragilaria* species, and *Encyonopis* species (*E. descripta* and *E. cesatii*). In addition to *Tabellaia* spp. the grass sample also consisted of *Gomphonema* species (mostly *G. parvulum*) and *Achnanthidium minutissimum,* while the benthic moss mat sample consisted of large *Navicula* species, *Encyonopsis* species and *Brachysira* species (*B. stryiaca* and *B. vitrea*) (Table 3). Chyrosphyte cyst abundances were generally low in the substrate samples (2 to 6%), except for submerged peat, which had higher abundances (26%). Protozoan plates were almost entirely absent in these samples (~0 to 0.25%) (Table 3).

4. Discussion

The peatland-dominated Scotty Creek basin is in a period of rapid transition due to climate warming and rapid loss of permafrost. The aim of this study was to characterize the present-day limnology and ecology of shallow lakes in or near Scotty Creek, and underlying drivers, as a benchmark from which to study future change. Spatial patterns in water chemistry, lake physical characteristics and diatom assemblages were explored in 16 lakes. For 9 of the 16 lakes where landscape classification data was available, the extent of fen and collapse scar coverage was explored as a driver of water chemistry. Lastly, loggers were deployed in First Lake and Goose Lake to gain a better understanding of seasonal dynamics in water depth, temperature, and oxygen.

4.1 Seasonal dynamics in Goose Lake and First Lake

Goose Lake and First Lake did not exhibit thermal stratification over the 76-day period the loggers were deployed. Paleolimnological records indicate that thermal stability has been increasing in lakes across the circumpolar Arctic in response to climate change (Rühland et al. 2015). Although stratification of shallow lakes is rare, it has been observed in shallow lakes with high DOC concentrations, as DOC can absorb more solar radiation and increase surface water temperatures (Bouchard et al. 2011; Deshpande et al. 2017). Shallow boreal lakes may also be more prone to periodic thermal stratification where trees provide shelter from wind mixing (Klaus et al. 2021).

Oxygen availability at the sediment-water interface is a fundamental control on lake biogeochemical cycling. For example, methanogenesis, the production of methane as a respiratory by-product, occurs in anoxic conditions, and may be fueled by the addition of terrestrial sources of organic carbon (Grasset et al. 2018). Increased stratification, in combination with increased bacterial consumption of high terrestrial carbon inputs, have resulted in prolonged periods of anoxia in some subarctic lakes in Northern Quebec (Desphande et al. 2017). Small subarctic lakes in Norway similarly experienced decreasing oxygen concentrations with increasing DOC inputs (Couture et al. 2015). These changes could have important consequences for the carbon cycle as increased export of terrestrial carbon and longer periods of stratification may result in shallow subarctic lakes becoming important emitters of methane (Grasset et al.

2018). In contrast, high DOC subarctic lakes in Siberia had oxygen concentrations at equilibrium with the atmosphere (Shirokova et al. 2013). Oxygen levels near the sediment-water interface in Goose Lake and First Lake ranged between 5 and 12.5 mg/L and would be considered low for the protection of aquatic life (for reference, 9.5 mg/L is considered the lowest acceptable dissolved oxygen concentration for early life stages; CCME 1991). As both Goose Lake and First Lake have high DOC concentrations (23.74 and 21.93 mg/L, respectively) high rates of microbial respiration may be responsible for lower oxygen levels, as there is no evidence of stratification.

Peatlands cover approximately 19% of the circumpolar permafrost region (Tarnocai et al. 2009), yet high resolution limnological data of these sites is scarce and is a notable gap in global lake monitoring networks such as GLEON (Global Lakes Ecological Observation Network). As permafrost wetland complexes near the southern extent of permafrost are particularly vulnerable to rising air temperatures, the Scotty Creek basin offers an ideal location for long-term limnological research. Lake monitoring data collected here can be combined with ongoing field, remote sensing, and modelling research at the Scotty Creek Research Station, to provide a more holistic understanding of changes in terrestrial-aquatic linkages with permafrost thaw.

4.2 Spatial patterns in lake water chemistry

We expected the relative proportion of collapse scars and channel fens within 250 m of the lake shoreline would be an important driver of water chemistry in the Scotty Creek basin, because of the differential roles these landscape features play in the biogeochemical processing and transport of materials from land to lake. In this landscape, channel fens act as water conveyors, while collapse scars act predominately as water storage (Quinton et al. 2019). Collapse scars may be important sources of chromophoric DOC, as they were identified in this study as having high DOC and high color (522 TCU). Our spatial results, however, showed limited evidence for the role of channel fens and collapse scars in driving lake water chemistry. For example, SC5 and SC8 were hydrologically isolated from the channel fen network, and both had high color, which may suggest that channel fens have a role in flushing terrestrial DOC from lakes; however, Next Lake also had relatively high color despite being well-connected hydrologically.

We postulate that temporal dynamics in a rapidly changing landscape could explain why we do not see strong spatial evidence for the importance of fen and collapse scar extent in influencing lake water chemistry. For example, an increase in fen development could initially increase color in lakes due to a phenomenon known as "bog capture" (Connon et al. 2014), where previously isolated collapse scar wetlands become connected to the expanding fen network as permafrost plateaus continue to degrade. The highly colored water is then conveyed to nearby lakes through the fen network. With time, colored DOC may ultimately be flushed from Next Lake and other lakes recently influenced by the capture of collapse scars. Paleolimnological approaches that reconstruct DOC trajectories in lakes in combination with a time series of remotely sensed images could be used in future studies to test this.

4.3 Diatom ecology in permafrost wetlands and lakes of the Scotty Creek basin

Two different diatom assemblages were observed in 13 of the 16 lakes sampled. The first assemblage, identified in 6 lakes, was comprised of small benthic Fragilariaceae and small *Navicula* species (*sensu lato)*, which were found in this study to be associated with higher color. A similar assemblage has been identified in a lake with high color located southeast of the Scotty Creek basin near Tathlina Lake (Coleman et al. 2015; Korosi et al. 2015). Small benthic Fragilariaceae have been used as indicators of harsher, low light conditions and tend to decrease in abundance with warming (Rühland et al. 2008; Bouchard et al. 2013). Although primarily benthic, they have also been identified as tychoplanktonic (e.g. Velez et al. 2021), and can be displaced into the water column with mixing; However, their absence in Goose Lake and First Lake, which appeared to be well mixed at least during the ice-free season of 2019, suggests that their presence is not related primarily to column mixing.

The second assemblage, recorded in 7 lakes, was comprised of *Encyonopsis* species and large *Navicula* species. These species were found to be associated with high DOC and lower pH (though note the pH gradient is narrow, ranging from 7.85 - 8.75). The species assemblages in these lakes were similar to the assemblage found in the benthic moss mat sampled from Goose Lake. While large *Navicula* species have been associated with higher DOC (Rühland et al. 2003, Coleman et al. 2015), *Encyonopsis* species are epiphytic and often associated with mosses (Bahls 2013). Therefore, a main driver of diatom assemblages in these lakes may be the presence of a benthic moss mat, which is dependent on light being able to penetrate to the benthic zone of these lakes. Colored DOC could have limited the growth of moss and associated epiphytes in these lakes. DOC has previously been shown to negatively impact benthic primary production in boreal lakes in Sweden and Alaska through light limitation (Seekell et al. 2015), though the study did not distinguish between DOC and lake color and aquatic plants are known to produce authochthonous, non-chromophoric DOC (Pagano et al. 2014). We infer autochthonous DOC sources from extensive moss and macrophyte growth to be the reason why our diatom epiphyte-dominated lakes exhibited high DOC but were generally lower in color. A better understanding of the interplay between lake depth, DOC, light, and benthic primary production is needed to predict the consequences of permafrost thaw on shallow lakes in boreal permafrost peatlands.

The species assemblages that were present in high abundances in wetlands were different from assemblages that were identified in lakes. Three of the most common species or groups of species, were *Eunotia* species, *Gomphonema* species, and *Tabellaria* spp. *Eunotia* species in particular are commonly identified in paleoecological studies using peat cores, and have lower pH optima (e.g. Hargan et al. 2015). *Tabellaria* spp have been found in a wide variety of freshwater habitats, including lakes and peatlands, and have broad morphological variations in terms of size, but shorter species/varieties as found here have often been observed in peatlands and attached to vegetation (DeColibus, 2013). This is consistent with the assemblages identified in the substrate samples, as *Tabellaria* spp. was found in high abundances in the grasses and submerged vegetation. The diatom assemblage identified in the collapse scar site was found to be different from both lakes and fens and was dominated by *Kobayasiella subtilissima* (95%). Hargan et al. (2015) also found that *K. subtilissima* had higher prevalence in collapse scar habitats. Collapse scars also have the highest abundance of cysts and protozoan plates compared to both fens and lakes.

The two different assemblages of diatoms that were identified in these shallow subarctic lakes are likely driven by relative differences in benthic to pelagic production, which is impacted by the ability of light to penetrate into the water column. As increasing colored DOC concentrations can reduce light penetration, paleolimnological studies using diatoms as paleoindicators may be useful for examining the trajectory of lake browning with continued permafrost thaw. The low abundances of common wetland species also identified in lakes suggests that we are not seeing a strong biological signal of these environments in the lakes. We can therefore be confident that the diatom assemblages recorded in lakes are indicative of that lake’s conditions and have not been transported from other locations. It is, however, important to note that changing lake depth and duration of the ice-free season may also influence the relative importance of benthic to pelagic production in lakes and decreases in lake depth are expected with drying of wetlands with on-going thaw and loss of permafrost (Chasmer and Hopkinson 2016; Carpino et al. 2021). This highlights the importance of continued high-resolution monitoring in addition to paleolimnological studies to better predict how these lakes will change with future warming in this dynamic landscape.

4.4 Summary of main findings and future directions

The Scotty Creek basin is experiencing a rapid loss of permafrost that manifests as wetland thermokarst, where ground subsidence results in the conversion of black spruce forest into wetlands and enhances watershed hydrological connectivity (Quinton et al. 2019). Given the differing roles that forested peat plateaus, channel fens, and collapse scars play in the transport and processing of DOC, we predicted that the degree of lake connection to the channel fen network could be related to lake chromophoric DOC, but this was not supported by our data. DOC and lake color, however, do appear to be key drivers of diatom assemblages in these lakes, with diatom assemblages tending to fall into one of two clusters. One cluster, comprised of small benthic Fragilariaceae and small *Navicula* species (*sensu lato*), was found associated with higher lake color, while the second cluster was comprised of epiphytic *Encyonopsis* and large *Navicula* species and was associated with high DOC, lower color, and the presence of a benthic moss mat. Future directions should explore DOC quality (and its drivers) in these lakes, and the interplay between DOC, lake depth, and light in structuring diatom assemblages and benthic primary production. Furthermore, as Scotty Creek is already in a period of rapid transition, long-term studies are needed to understand the trajectories and mechanisms of limnological change. First Lake and Goose Lake present ideal candidate sites for the establishment of a long-term limnological monitoring program, and the close association between diatoms and lake DOC/color indicate that diatoms will be useful paleoecological indicators of changes in lake carbon and primary production dynamics in future studies.

Acknowledgements

We would like to thank Arnab Shuvo for assistance in the field, Kristine Haynes and Mason Dominico for providing precipitation data and Emily Stewart for reviewing this manuscript and providing advice. This research was supported by a Natural Sciences and Engineering Research Council of Canada (NSERC) Discovery and Northern Supplement to JBK, and an NSERC postgraduate scholarship and Weston Family Foundation scholarship to KAC. Fieldwork funding and logistical support was also provided by ArcticNet, the Polar Continental Shelf Program and the Northern Scientific Training Program. Scotty Creek is within the traditional territory of the Liidlii Kue First Nation (LKFN). Mahsi to the LKFN and the Dehcho First Nations for their support and leadership in scientific research at Scotty Creek.

The authors report that there are no competing interests to declare

Data associated with this manuscript are available through the York University Yorkspace Institutional Repository at http://hdl.handle.net/10315/39723

References

APHA. 1998. Standard Methods for the Examination of Water and Wastewater. 20th Edition, American Public Health Association, American Water Works Association and Water Environmental Federation, Washington DC.

APHA. 2011. Standard methods for the examination of water and wastewater, 22nd edn. American Public Health Association, Washington, DC

Bahls L. 2013. *Encyonopsis* from western North America: 31 species from Alberta, Idaho, Montana, Oregon, South Dakota, and Washington, including 17 species described as new. Northwest Diatoms, Volume 5. The Montana Diatom Collection, Helena, 46 pp.

Battarbee RW, Jones VJ, Flower RJ, Cameron NG, Bennion H, Carvalho L, Juggins S. 2001. Diatoms. In: Smol J.P., Birks H.J.B. & Last W.M. (eds.), Tracking environmental change using lake sediments, vol. 3: Terrestrial, algal, and siliceous indicators, Kluwer Academic Press, Dordrecht, The Netherlands, pp. 155–202.

Bouchard F, Francus P, Pienitz R, Laurion I. 2011. Sedimentology and geochemistry of thermokarst ponds in discontinuous permafrost, subarctic Quebec, Canada. Journal of Geophysical Research: Biogeosciences, 116(G2).

Bouchard F, Pienitz R, Ortiz JD, Francus P, Laurion I. 2013. Palaeolimnological conditions inferred from fossil diatom assemblages and derivative spectral properties of sediments in thermokarst ponds of subarctic Quebec, Canada. Boreas 42: 575–595.

Carpino O, Haynes K, Connon R, Craig J, Devoie É, Quinton W. 2021. Long-term climate-influenced land cover change in discontinuous permafrost peatland complexes. Hydrol. Earth Syst. Sci. 25(6):3301-3317.

CCME, Canadian Council of Ministers of the Environment. 1999. Canadian water quality guidelines for the protection of aquatic life: Dissolved oxygen (freshwater). In: Canadian environmental quality guidelines, 1999, Canadian Council of Ministers of the Environment, Winnipeg.

Chasmer L, Hopkinson C, 2017. Threshold loss of discontinuous permafrost and landscape evolution. Glob. Change Biol. 23(7): 2672-2686.

Chasmer L, Hopkinson C, Veness T, Quinton W, Baltzer J. 2014. A decision-tree classification for low-lying complex land cover types within the zone of discontinuous permafrost. Remote Sens. Environ. 143: 73-84.

Cole JJ, Carpenter SR, Pace ML, Van de Bogert MC, Kitchell JL, Hodgson JR. 2006. Differential support of lake food webs by three types of terrestrial organic carbon. Ecology Letters, 9: 558-568.

Cole JJ, Prairie YT, Caraco NF, McDowell WH, Tranvik LJ, Striegl RG, Duarte CM, Kortelainen P, Downing JA, Middelburg JJ, Melack J. 2007. Plumbing the global carbon cycle: integrating inland waters into the terrestrial carbon budget. Ecosystems, 10: 172-185.

Coleman KA, Korosi JB. 2023. Dataset: (Paleo)limnological data for small, shallow lakes at or near the Scotty Creek Research Station in the Dehcho region (Northwest Territories, Canada). http://hdl.handle.net/10315/39723

Coleman KA, Palmer MJ, Korosi JB, Kokelj SV, Jackson K, Hargan KE, Courtney Mustaphi CJ, Thienpont JR, Kimpe LE, Blais JM, Pisaric MFJ, Smol JP. 2015. Tracking the impacts of recent warming and thaw of permafrost peatlands on aquatic ecosystems: a multi-proxy approach using remote sensing and lake sediments. Boreal Environ Res, 20: 363-377.

Connon RF, Quinton WL, Craig JR, Hayashi M. 2014. Changing hydrologic connectivity due to permafrost thaw in the lower Liard River valley, NWT, Canada. Hydrol. Process. 28: 4163–4178.

Couture RM, de Wit HA, Tominaga K, Kiuru P, Markelov I. 2015. Oxygen dynamics in a boreal lake responds to long-term changes in climate, ice phenology, and DOC inputs. J. Geophys. Res. Biogeosci. 120: 2441–2456.

DeColibus D. 2013. Tabellaria flocculoda. In Diatoms of North America. Retrieved July 10, 2021, from https://diatoms.org/species/tabellaria_flocculosa

Deshpande BN, Maps F, Matveev A, Vincent WF. 2017. Oxygen depletion in subarctic peatland thaw lakes. Arct. Sci. 1: 1-23

Disher BS, Connon RF, Haynes KM, Hopkinson C, Quinton WL. 2021. The hydrology of treed wetlands in thawing discontinuous permafrost regions. Ecohydrology, p.e2296.

Fallu MA, Allaire N, Pienitz R. 2002. Distribution of freshwater diatoms in 64 Labrador (Canada) lakes: species-environment relationships along latitudinal gradients and reconstruction models for water color and alkalinity. Can. J. Fish. Aquat. Sci. 59: 329–349

Frey KE, McClelland JW. 2009. Impacts of permafrost degradation on arctic river biogeochemistry. Hydrol Process., 23(1): 169-182.

Glew JR. 1988. A portable extruding device for close interval sectioning of unconsolidated core samples. J. Paleolimnol. 1(3): 235-239.

Gordon J, Quinton W, Branfireun BA, Olefeldt, D. 2016. Mercury and methylmercury biogeochemistry in a thawing permafrost wetland complex, Northwest Territories,

Canada. Hydrol Process., 30: 3627-3638.
Guiry MD, Guiry GM. 2021. *AlgaeBase*. World-wide electronic publication, National University of Ireland, Galway. https://www.algaebase.org; searched on 06 July 2021.
Hargan KE., Rühland KM, Paterson AM, Finkelstein SA, Holmquist JR, MacDonald GM, Keller W, Smol JP. 2015. The influence of water-table depth and pH on the spatial distribution of diatom species in peatlands of the Boreal Shield and Hudson Plains, Canada. Botany, 93: 57–74.
Harrell FE. 2021. Hmisc: Harrell Miscellaneous. R package version 4.5-0. https://CRAN.R-project.org/package=Hmisc
Harris LI, Richardson K, Bona KA, Davidson SJ, Finkelstein SA, Garneau M, McLaughlin J, Nwaishi F, Olefeldt D, Packalen M., Roulet NT. 2022. The essential carbon service provided by northern peatlands. Front. Ecol. Environ., 20: 222-230.
Hugelius G, Loisel J, Chadburn S, Jackson RB, Jones M, MacDonald G, Marushchak M, Olefeldt D, Packalen M, Siewert MB, Treat C. 2020. Large stocks of peatland carbon and nitrogen are vulnerable to permafrost thaw. Proc. Nat. Acad. Sci., 117: 20438-20446.
Ivanov K, Zaprjanova P, Petkova M, Stefanova V, Kmetov V, Georgieva D, Angelova V. 2012. Comparison of inductively coupled plasma mass spectrometry and colorimetric determination of total and extractable phosphorus in soils. Spectrochimica Acta Part B: At. Spectrosc., 71: 117-122.
Karlsson JM, Lyon SW, Destouni G. 2012. Thermokarst lake, hydrological flow and water balance indicators of permafrost change in Western Siberia. J. Hydrol.464: 459–466.
Kettles I, and Tarnocai C. 1999. Development of a model for estimating the sensitivity of

Canadian peatlands to climate warning. Géographie physique et Quaternaire, 53(3), pp.323-338.

Klaus M, Karlsson J, Seekell D. 2021. Tree line advance reduces mixing and oxygen concentrations in arctic-alpine lakes through wind sheltering and organic carbon supply. Glob. Change Biol., **27**, 4238– 4253.

Korosi JB, McDonald J, Coleman KA, Palmer MJ, Smol JP, Simpson MJ, Blais JM. 2015. Long-term changes in organic matter and mercury transport to lakes in the sporadic discontinuous permafrost zone related to peat subsidence. Limnol Oceanogr. 60(5): 1550-1561.

Krammer K, Lange-Bertalot H. 1997. *Bacillariophyceae 2. Teil: Bacillariaceae, Epithemiaceae, Surirellaceae*. Süßwasserflora von Mitteleuropa 2/2. Spektrum Akademischer Verlag, Berlin, Germany.

Krammer K, Lange-Bertalot H. 1999. *Bacillariophyceae 1. Teil: Naviculaceae. Süßwasserflora von Mitteleuropa 2/1*. Spektrum Akademisher Verlag, Berlin, Germany.

Krammer K, Lange-Bertalot H. 2000. *Bacillariophyceae 3. Teil: Centrales, Fragilariaceae, Eunotiaceae. Süßwasserflora von Mitteleuropa 2/3*. Spektrum Akademischer Verlag, Berlin, Germany.

Mack M, Connon R, Makarieva O, McLaughlin J, Nesterova N., Quinton, W. 2021. Heterogenous runoff trends in peatland-dominated basins throughout the circumpolar North. Environ. Res. Comms., 3: 075006.

Michelutti N, Holtham AJ, Douglas MSV, Smol JP. 2003. Periphytic diatom assemblages from ultra-oligotrophic and UV transparent lakes and ponds on Victoria Island and comparisons with other diatom surveys in the Canadian arctic. J. Phycol. 39: 465–480.

O'Neill HB, Wolfe SA, Duchesne C. 2019. New ground ice maps for Canada using a paleogeographic modelling approach. Cryosphere 13: 753–773.

Oksanen J, Blanchet FG, Friendly M, Kindt R, Legendre P, McGlinn D, Minchin PR, O'hara RB, Simpson GL, Solymos P, Stevens MHH. 2019. Vegan: community ecology package (version 2.5-6). *The Comprehensive R Archive Network*.

Pagano T, Bida M, Kenny J. 2014. Trends in Levels of Allochthonous Dissolved Organic Carbon in Natural Water: A Review of Potential Mechanisms under a Changing Climate. Water. 6: 2862–2897.

Pienitz R, Smol JP, MacDonald G.M. 1999. Paleolimnological reconstruction of Holocene climatic trends from two boreal treeline lakes, Northwest Territories, Canada. Arct. Antarct. Alp. Res. 31: 82-93.

Porcal P, Koprivnjak JF, Molot LA, Dillon PJ. 2009. Humic substances—part 7: the biogeochemistry of dissolved organic carbon and its interactions with climate change. Environ. Sci. Pollut. Res.16: 714–726.

Quinton W, Berg A, Braverman M, Carpino O, Chasmer L, Connon R, Craig J, Devoie É, Hayashi M, Haynes K, Olefeldt D. 2019. A synthesis of three decades of hydrological research at Scotty Creek, NWT, Canada. Hydrol. Earth Syst. Sci. 23(4): 2015-2039.

Quinton WL, Hayashi M, Chasmer LE. 2011. Permafrost-thaw-induced land-cover change in the Canadian subarctic: implications for water resources. Hydrol. Process.25, 152–158.

R Core Team. 2020. R: *A language and environment for statistical computing.* Vienna: R foundation for Statistical Computing.

Rühland K, Priesnitz A, Smol JP. 2003. Paleolimnological evidence from diatoms for recent environmental changes in 50 lakes across Canadian Arctic treeline. Arct. Antarct. Alp.

Res. 35(1): 110-123.

Rühland K, Paterson AM, Smol JP. 2015. Diatom assemblage responses to warming: reviewing the evidence. J. Paleolimnology 54: 1-35

Seekell DA, Lapierre JF, Ask J, Bergström AK, Deininger A, Rodríguez P, Karlsson J. 2015. The influence of dissolved organic carbon on primary production in northern lakes. Limnol. Oceanogr. Lett. 60(4): 1276-1285.

Shirokova LS, Pokrovsky OS, Kirpotin SN, Desmukh C, Pokrovsky BG, Audry S, Viers J. 2013. Biogeochemistry of organic carbon, CO_2, CH_4, and trace elements in thermokarst water bodies in discontinuous permafrost zones of Western Siberia. Biogeochemistry. 113: 573–593.

Sim TG, Swindles GT, Morris PJ, Baird AJ, Cooper CL, Gallego-Sala AV, Charman DJ, Roland TP, Borken W, Mullan DJ, Aquino-Lopez MA. 2021. Divergent responses of permafrost peatlands to recent climate change. Environ. Res. Lett., 16: 034001.

Smith LC, Pavelsky TM, MacDonald GM, Shiklomanov AI, Lammers RB. 2007. Rising minimum daily flows in northern Eurasian rivers: A growing influence of groundwater in the high-latitude hydrologic cycle. J. Geophys. Res. Biogeosci.112

Spaulding SA, Potapova MG, Bishop IW, Lee SS, Gasperak TS, Jovanoska E, Furey PC, Edlund MB. 2021. Diatoms. org: supporting taxonomists, connecting communities. Diatom Research. 36(4): 291-304

Spence C, Norris M, Bickerton G, Bonsal BR, Brua R, Culp JM, Dibike Y, Gruber S, Morse PD, Peters DL, Shrestha R. 2020. The Canadian Water Resource Vulnerability Index to Permafrost Thaw (CWRVIPT). Arct. Sci., 6(4), pp.437-462

SOCR, State of the Cryosphere Report: A needed decade of urgent action. 2021.

www.iccinet.org/statecryo21

Tanentzap AJ, Kielstra BW, Wilkinson GM, Berggren M, Craig N, Del Giorgio PA, Grey J, Gunn JM, Jones SE, Karlsson J, Solomon CT, Pace ML. 2017. Terrestrial support of lake food webs: Synthesis reveals controls over cross-ecosystem resource use. Sci. Adv., 3: e1601765.

Tank SE, Vonk JE, Walvoord MA, McClelland JW, Laurion I, Abbott BW. 2020. Landscape matters: Predicting the biogeochemical effects of permafrost thaw on aquatic networks with a state factor approach. Permafr. Periglac. Process. 31: 358-370.

Tarnocai C, Canadell CJG, Schuur EAG, Kuhry P, Mazhitova G, Zimov S. 2009. Soil organic carbon pools in the northern circumpolar permafrost region. Global Biogeochem. Cycles. 23: GB2023,

Thienpont JR, Rühland KM, Pisaric MF, Kokelj SV, Kimpe LE, Blais JM, Smol JP. 2013. Biological responses to permafrost thaw slumping in Canadian Arctic lakes. Freshw. Biol. 58: 337-353.

Vonk JE, Alling V, Rahm L, Mörth CM, Humborg C, Gustafsson Ö. 2012. A centennial record of fluvial organic matter input from the discontinuous permafrost catchment of Lake Torneträsk. J. Geophys. Res.: Biogeosci. 117 (G3).

Vonk JE, Mann PJ, Davydov S, Davydova A, Spencer RGM, Schade, J., Sobczak, W.V., Zimov, N., Zimov, S., Bulygina, E., Eglinton, T.I., Holmes, R.M., 2013. High biolability of ancient permafrost carbon upon thaw. Geophys. Res. Lett. 40: 2689–2693.

Vonk JE, Tank SE, Bowden WB, Laurion I, Vincent WF, Alekseychik P, Amyot M, Billet MF, Canario J, Cory RM, Deshpande BN. 2015. Reviews and syntheses: Effects of permafrost thaw on Arctic aquatic ecosystems. Biogeosciences. 12(23): 7129-7167.

Vonk JE, Tank SE, Walvoord MA. 2019. Integrating hydrology and biogeochemistry across frozen landscapes. Nat. Comm. 10: 1-4.

Wauthy M, Rautio M, Christoffersen KS, Forsström L, Laurion I, Mariash HL, Peura S, Vincent WF. 2018. Increasing dominance of terrigenous organic matter in circumpolar freshwaters due to permafrost thaw: Increasing allochthony in arctic freshwaters. Limnol Oceanogr Letters 3: 186–198.

Wickham et al., (2019). Welcome to the tidyverse. Journal of Open Source Software, 4(43), 1686

Zhang T, Barry RG, Knowles K, Heginbottom JA, Brown J. 1999. Statistics and characteristics of permafrost and ground ice distribution in the Northern Hemisphere. Polar Geography, 23(2): 132–154.

Zhang TJ, Frauenfeld OW, Serreze MC, Etringer A, Oelke C, McCreight J, Barry RG, Gilichinsky D, Yang DQ, Ye HC, Ling F, Chudinova S. 2005. Spatial and temporal variability in active layer thickness over the Russian Arctic drainage basin. J Geophys Res- Atmospheres, 110: D16101.

Table 1: Physical characteristics and modern water chemistry statistics for 16 lakes in the Scotty Creek and surrounding basins, collected July 2018.

	Mean	**± SD**	**Min**	**Max**	**Median**
Depth (m)	1.3	0.4	0.9	2.1	1.2
Area (km^2)	1.06	1.69	0.11	7.13	0.32
Shoreline Development Index	1.18	0.21	1.02	1.75	1.09
pH	8.23	0.27	7.85	8.75	8.20
DOC (mg/L)	18.79	3.13	12.96	23.74	18.35
True Color (TCU)	176	124	18	463	174
TP (µg/L)(unfiltered)	18.3	7.9	8.0	38.0	17.0
TN (mg/L)(filtered)	0.90	0.28	0.54	1.54	0.79
Conductivity (µS/cm)	106.9	58.5	55.5	244.2	83.1
Alkalinity ($CaCO_3$)(mg/L)	54	29	28	124	43
Calcium (mg/L)	15.4	6.5	7.9	29.8	13.3
Potassium (mg/L)	0.61	0.65	0.19	2.49	0.34
Lithium (µg/L)	1.4	0.8	0.7	3.2	1.2
Magnesium (mg/L)	4.67	3.08	2.24	12.70	3.51
Manganese (µg/L)	17.3	8.3	4.9	35.1	15.5
Sodium (mg/L)	2.35	1.93	0.74	7.25	1.62
Silicon (mg/L)	1.52	0.98	0.27	4.33	1.21
Strontium (µg/L)	61.1	36.0	28.5	149.0	45.3

SD = standard deviation; Area = surface area; DOC = dissolved organic carbon; TP = total phosphorus; TN = total dissolved nitrogen

Table 2: Spearman’s correlation coefficients of water chemistry variables and physical lake characteristics for 16 lakes in the Scotty Creek basin. *p<0.05, **p<0.01

	Area	**D_L**	**pH**	**DOC**	**TP**	**TN**	**Color**	**Cond**	**Alk**	**Ca**	**K**	**Li**	**Mg**	**Mn**	**Na**	**Sr**
Area	1.00	0.45	0.21	-0.06	-0.07	0.54	-0.85**	0.79**	0.85**	0.74**	0.78**	0.29	0.77**	0.52	0.36	0.57*
D_L		1.00	-0.07	0.12	-0.19	0.22	-0.23	0.50*	0.47	0.43	0.35	0.35	0.48	0.12	0.30	0.42
pH			1.00	-0.16	0.10	0.45	-0.54	0.48	0.46	0.37	0.63**	0.16	0.51*	0.48	0.42	0.49
DOC				1.00	0.58*	0.52*	0.16	-0.01	-0.06	-0.01	-0.06	0.17	-0.04	0.22	-0.02	-0.04
TP					1.00	0.48	-0.06	-0.21	-0.11	-0.28	-0.05	0.20	-0.20	0.51*	0.29	-0.21
TN						1.00	-0.69**	0.53	0.52*	0.49	0.65**	0.50*	0.51*	0.52*	0.53*	0.58*
Color							1.00	-0.76**	-0.81**	-0.68**	-0.84**	-0.38	-0.74**	-0.54*	-0.55*	-0.65**
Cond								1.00	0.94**	0.95**	0.83**	0.32	0.99**	0.54*	0.33	0.80**
Alk									1.00	0.89**	0.85**	0.36	0.95**	0.57*	0.48	0.76**
Ca										1.00	0.74**	0.37	0.94**	0.47	0.28	0.86**
K											1.00	0.19	0.84**	0.43	0.44	0.75**
Li												1.00	0.29	0.29	0.82**	0.55*
Mg													1.00	0.52*	0.37	0.77**
Mn														1.00	0.27	0.29
Na															1.00	0.51*
Sr																1.00

Area = Surface area; D_L = shoreline development index; DOC = dissolved organic carbon; TP = total phosphorus; TN = total dissolved nitrogen; Color = true color; Cond = conductivity; Alk = alkalinity; Ca = calcium; K = potassium; Li = lithium; Mg = magnesium; Mn = manganese; Na = sodium; Sr = strontium

Table 3: Dominant diatom species identified in lake substrate samples. Percentage of chrysophyte cysts and protozoan plates, in relation to diatom valves, also included.

	Sediment	Submerged Peat	Grasses	Submerged vegetation	Benthic Moss Mat
Location	Shoreline	Shoreline	Shoreline	Shoreline	~ 1 m depth, north basin
Dominant Diatoms	Large *Navicula* (~38%)	Large *Navicula* (~30%)	*Tabellaria* spp (~48%)	*Tabellaria* spp (~71%)	Large *Navicula* spp (~39%)
	Planktonic *Fragilaria* (~9%)	*Tabellaria* spp (~11%)	*Gomphonema* spp (~21%)		*Encyonopsis* spp (~14%)
	Encyonema spp (~8%)	Planktonic *Fragilaria* (~9%)	*Achnanthidium minutissimum* (~11%)		*Brachysira* spp (~11%)
	Brachysira (~7%)	*Encyonopsis* spp (~9%)			*Achnanthes* spp (~10%)
Cysts	Cysts (%): 4%	Cysts (%): 26%	Cysts (%): 2%	Cysts (%): 2%	Cysts (%): 6%
Protozoan Plates	Plates (%): 0.24%	Plates (%): 0%	Plates (%): 0%	Plates (%): 0%	Plates (%): 0.25%

Figure Captions

Figure 1. Map of study area: the Scotty Creek Basin, Northwest Territories, Canada. (A) Approximate location of site within Canada, (B) approximate location of site within Taiga Plains ecozone, (C) location of all study lakes, (D) true color image using Sentinel 2A data (accessed June 2021) of study lakes highlighted in (C) and includes wetland sample sites (white dots). Yellow markers are locations of data loggers.

Figure 2. Lake depth, temperature, dissolved oxygen and light absorption recorded every 30 minutes from June 7th to August 22nd 2019 from Goose Lake's north basin (A), Goose Lake's main basin (B) and First Lake (C). Precipitation data was recorded from Pluvio totalizing station located near Goose Lake.

Figure 3. Land classifications of the Scotty Creek basin based on classifications established in Chasmer et al. (2014). 250 m buffer zones are added to each lake, with the bog and fen environments within the buffer zones shown in red and yellow, respectively. Inset shows an example of the 250 m buffer zone around lake SC3, in detail.

Figure 4: Principal components analysis (PCA) of select water chemistry variables and physical characteristics of 16 shallow lakes in the Scotty Creek basin (A) and select water chemistry variables and areal proportion of collapse scar environment (Bog250m) and fen environment (Fen250m) within 250 m of lakes shorelines for 9 lakes included in landscape classification analyses (B). Dashed lines represent variables plotted passively. Area = lake area, D_L = shoreline development index.

Figure 5: Relative abundance diagram displaying the most common diatom taxa in the modern sediments retrieved from 16 shallow lakes in the Scotty creek and neighbouring basins. Species were grouped based on similar ecology. Species or ecological groups present at less than 2% relative abundance are not shown. Lakes were ordered using diatom PCA axes scores. Ratio of chrysophyte cysts to diatom valves and protozoan plates to diatom valves are also displayed.

Figure 6: Redundancy analysis (RDA) ordination triplot illustrating relationships between diatom species and environmental variables. Environmental variables are represented by arrows. Lake sites are in black. Diatoms species codes (red) are listed in Appendix A.

Figure 7: Ground-level photographs of wetland sites and corresponding list of dominant diatom species identified in a sample retrieved from the site. Percentage of chrysophyte cysts and protozoan plates, in relation to diatom valves, are also listed.

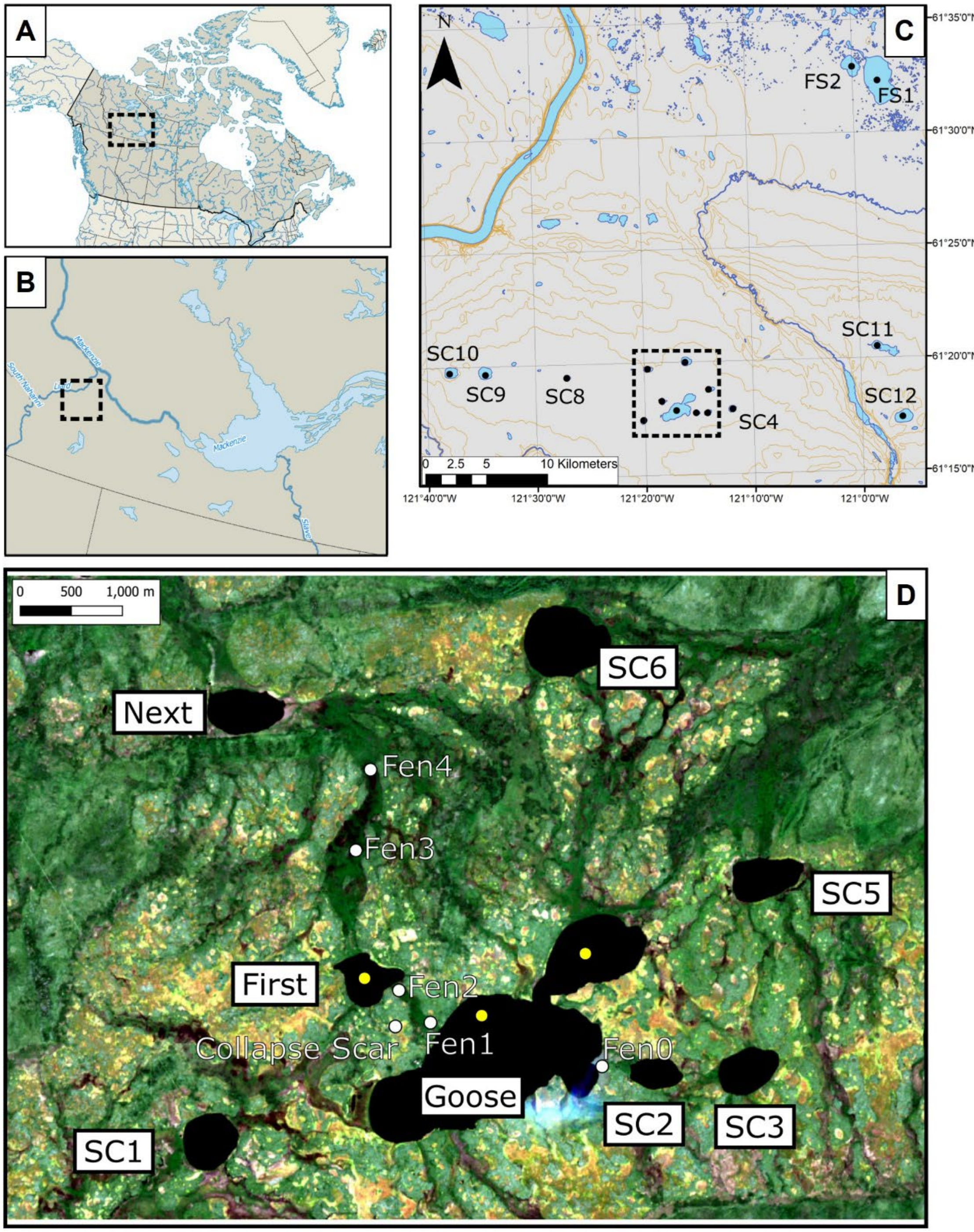
A
B
C
N
FS2
FS1
SC11
SC10
SC9
SC8
SC12
SC4
0 2.5 5 10 Kilometers
61°35'0"N
61°30'0"N
61°25'0"N
61°20'0"N
61°15'0"N
121°40'0"W
121°30'0"W
121°20'0"W
121°10'0"W
121°0'0"W
D
0 500 1,000 m
SC6
Next
Fen4
Fen3
SC5
First
Fen2
Collapse Scar
Fen1
Fen0
Goose
SC2
SC3
SC1

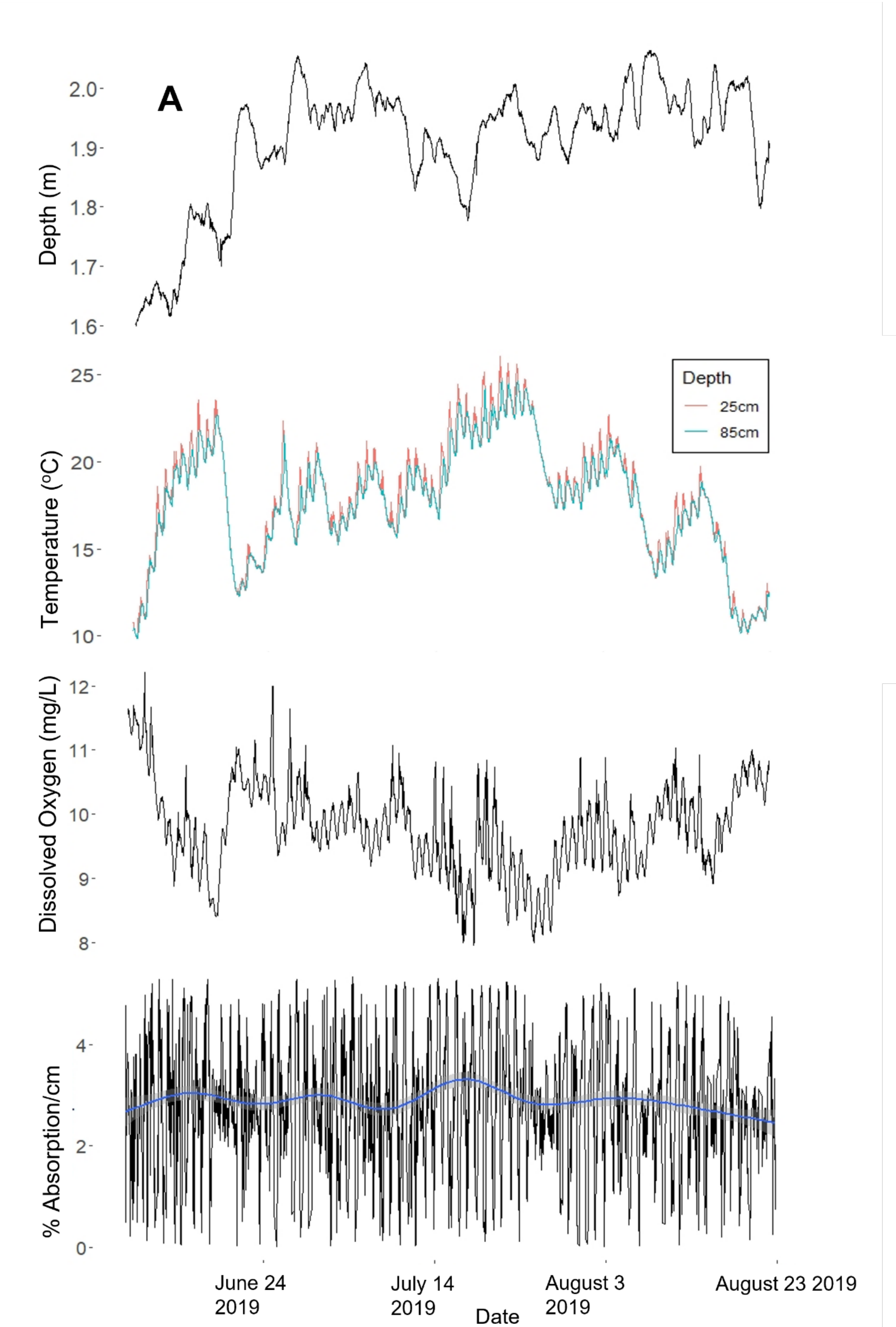

A
Depth (m)
2.0
1.9
1.8
1.7
1.6
Depth
25cm
85cm
Temperature (°C)
25
20
15
10
Dissolved Oxygen (mg/L)
12
11
10
9
8
% Absorption/cm
4
2
0
June 24
2019
July 14
2019
August 3
2019
August 23 2019
Date

830

831

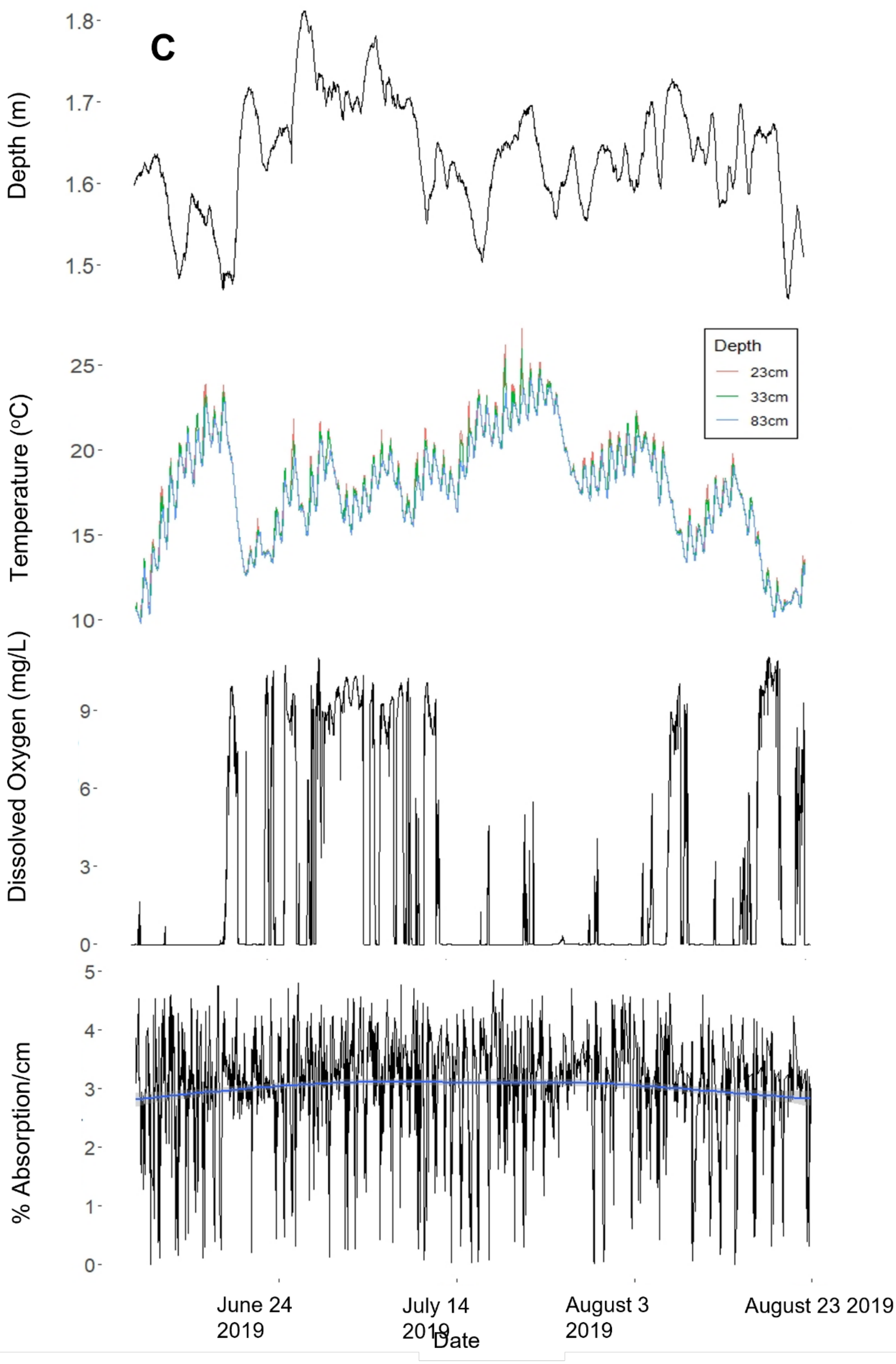
C
Depth (m)
1.8
1.7
1.6
1.5
Temperature (ºC)
25
20
15
10
Depth
23cm
33cm
83cm
Dissolved Oxygen (mg/L)
9
6
3
0
% Absorption/cm
5
4
3
2
1
0
June 24 2019
July 14 2019
August 3 2019
August 23 2019
Date

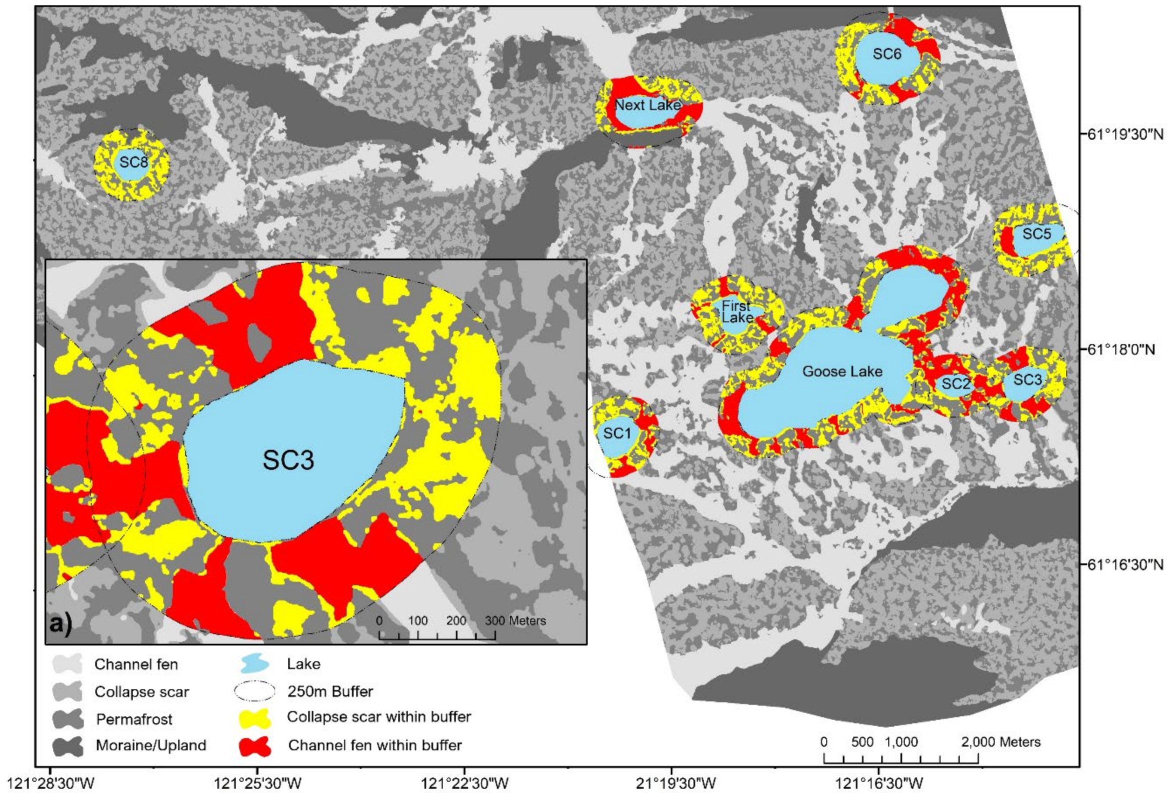
SC6
Next Lake
SC8
SC5
First Lake
Goose Lake
SC2
SC3
SC1
SC3
a)
0 100 200 300 Meters
Channel fen
Collapse scar
Permafrost
Moraine/Upland
Lake
250m Buffer
Collapse scar within buffer
Channel fen within buffer
0 500 1,000 2,000 Meters
61°19'30"N
61°18'0"N
61°16'30"N
121°28'30"W
121°25'30"W
121°22'30"W
21°19'30"W
121°16'30"W

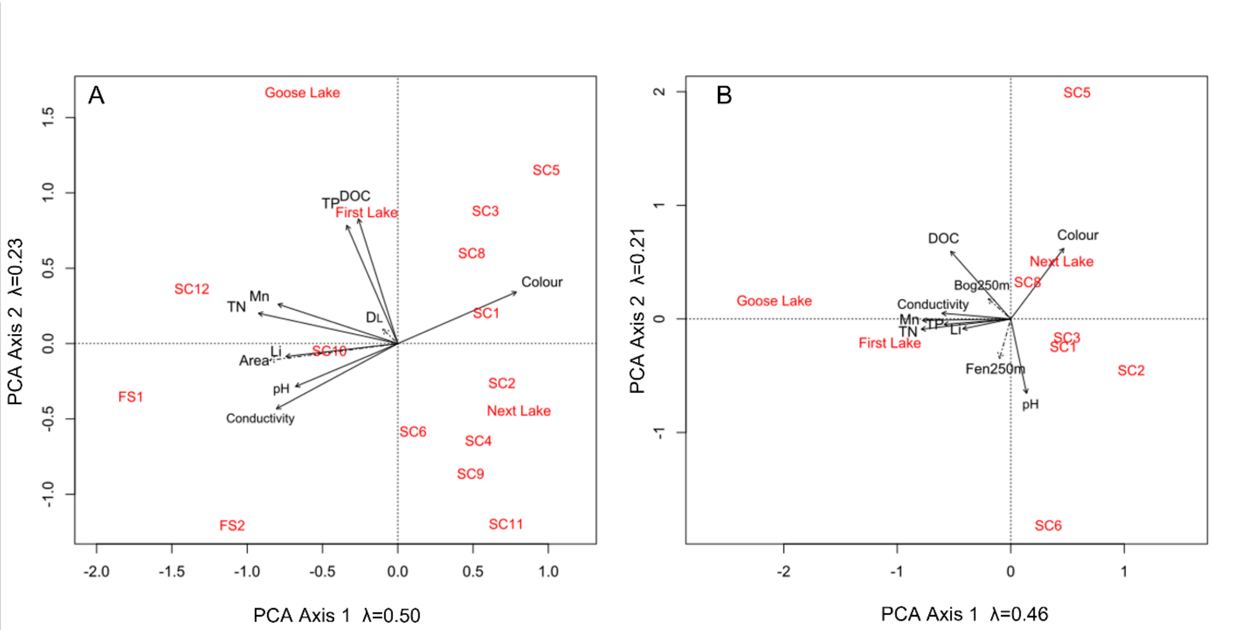
A
Goose Lake
SC5
SC3
TP
DOC
First Lake
SC8
SC12
Mn
TN
DL
Colour
SC1
Li
Area
SC10
FS1
pH
Conductivity
SC2
Next Lake
SC6
SC4
SC9
FS2
SC11
PCA Axis 1 λ=0.50
PCA Axis 2 λ=0.23
B
SC5
DOC
Colour
Next Lake
Bog250m
SC8
Goose Lake
Conductivity
Mn
TN
TP
Li
First Lake
SC3
SC1
SC2
Fen250m
pH
SC6
PCA Axis 1 λ=0.46
PCA Axis 2 λ=0.21

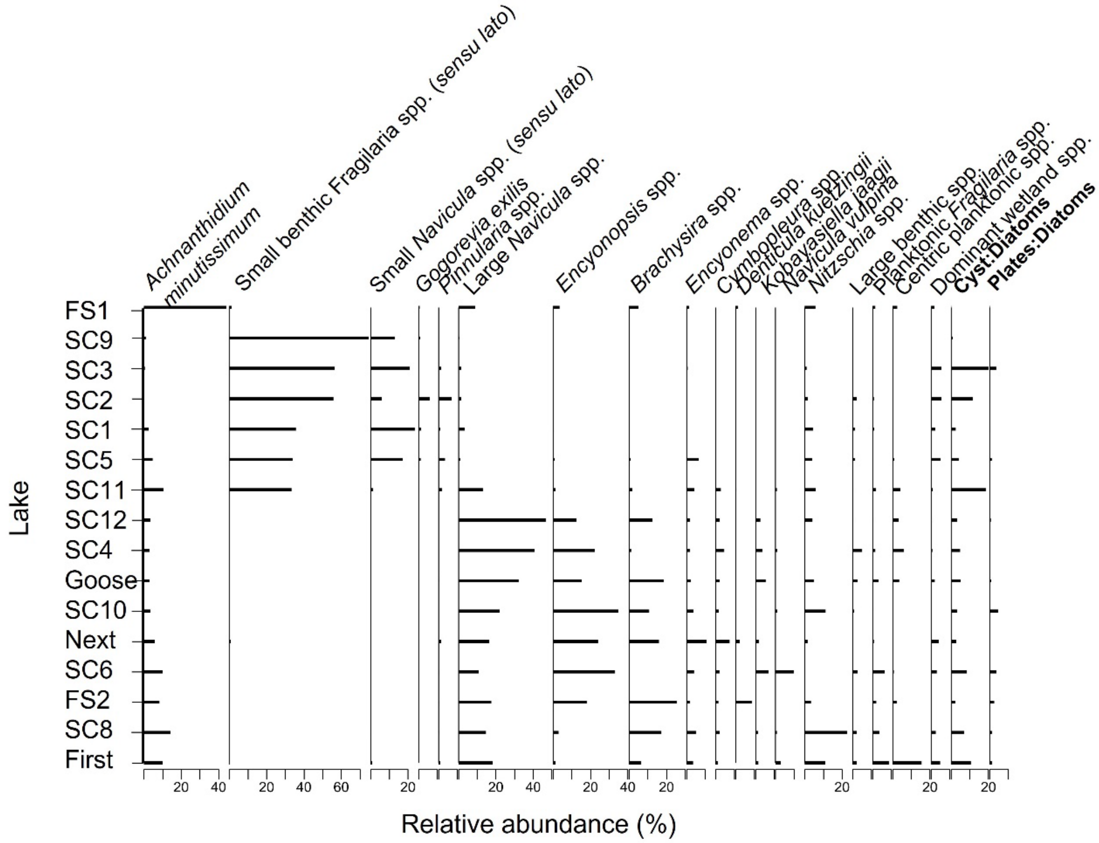
Achnanthidium minutissimum
Small benthic Fragilaria spp. (sensu lato)
Small Navicula spp. (sensu lato)
Gogorevia exilis
Pinnularia spp.
Large Navicula spp.
Encyonopsis spp.
Brachysira spp.
Encyonema spp.
Cymbopleura spp.
Denticula kuetzingii
Kobayasiella jaagii
Navicula vulpina
Nitzschia spp.
Large benthic spp.
Planktonic Fragilaria spp.
Centric planktonic spp.
Dominant wetland spp.
Cyst:Diatoms
Plates:Diatoms
Lake
FS1
SC9
SC3
SC2
SC1
SC5
SC11
SC12
SC4
Goose
SC10
Next
SC6
FS2
SC8
First
20
40
60
Relative abundance (%)

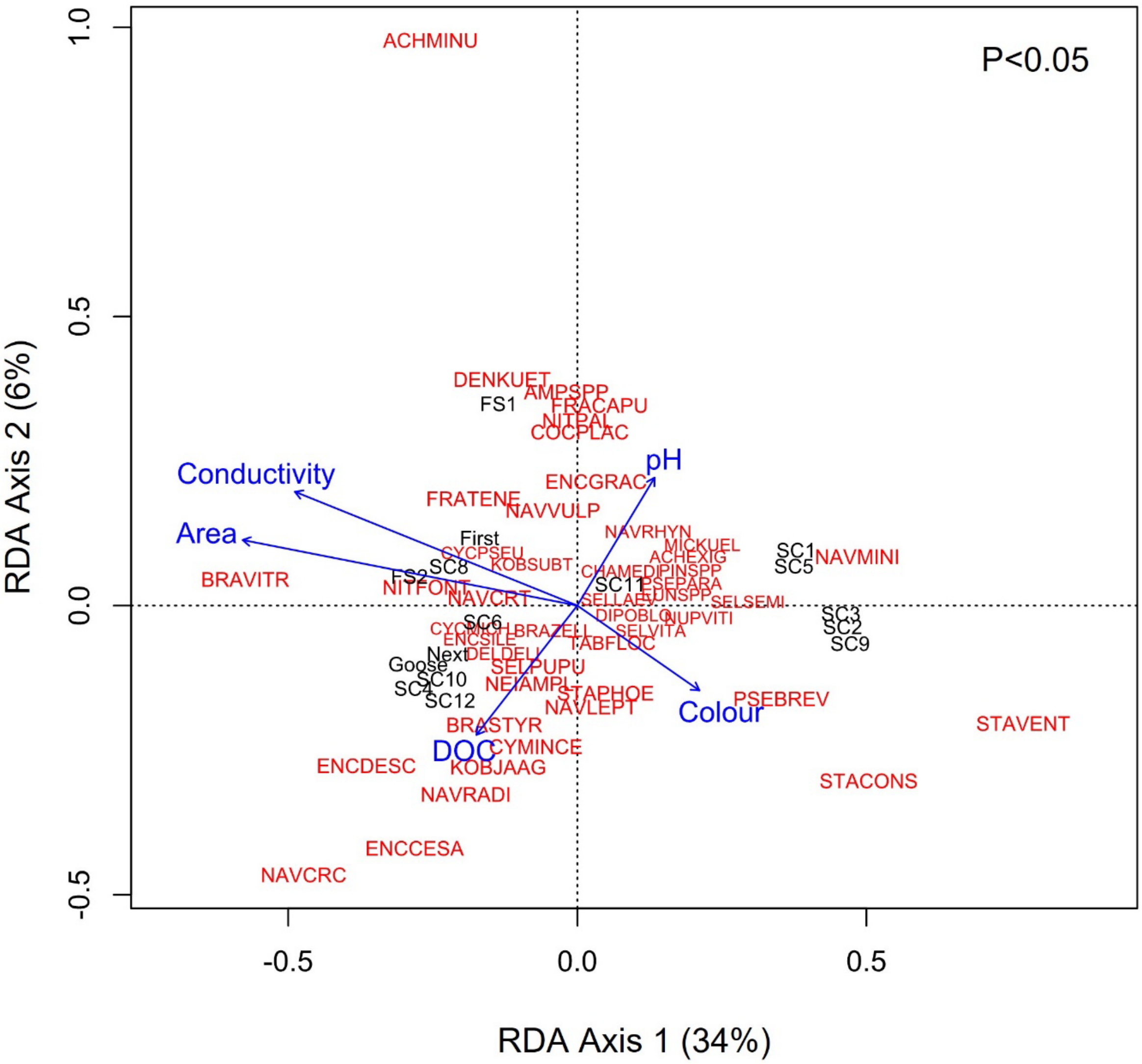
P<0.05
RDA Axis 2 (6%)
RDA Axis 1 (34%)
1.0
0.5
0.0
-0.5
-0.5
0.0
0.5
ACHMINU
DENKUET
AMPSPP
FS1
FRACAPU
NITPAL
COCPLAC
pH
Conductivity
ENCGRAC
FRATENE
NAVVULP
Area
First
NAVRHYN
MICKUEL
ACHEXIG
SC1
NAVMINI
SC5
SC8
KOBSUBT
BRAVITR
FS2
NITFONT
NAVCRT
SC11
SELSEMI
SC3
SC2
SC9
SC6
DIPOBLO
NUPVITI
SELVITA
ENCSILE
Next
Goose
SC10
SC4
SC12
SELPUPU
STAPHOE
NAVLEPT
PSEBREV
Colour
STAVENT
BRASTYR
DOC
CYMINCE
ENCDESC
KOBJAAG
STACONS
NAVRADI
ENCCESA
NAVCRC

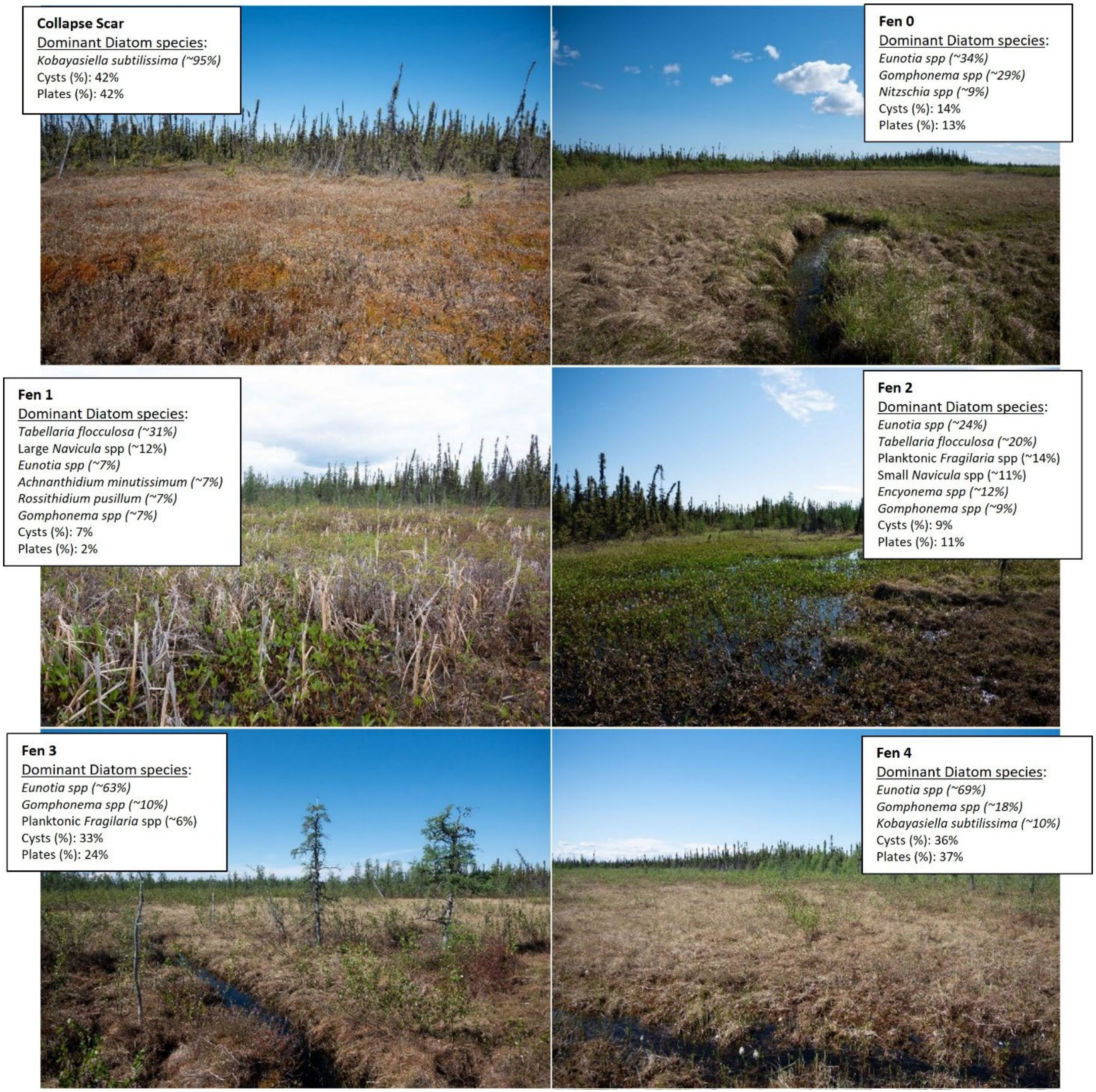

Appendices

Appendix A. List of diatom species groupings included in relative frequency diagram and taxon codes used in RDA. Species present in low abundances (<2%) were not includes in the RDA. Some genera were grouped for RDA analysis (*Pinnularia* spp., *Eunotia* spp., *Amphora* spp.).

Groupings in relative frequency diagram	Species	Taxon Code
Small benthic Fragilariaceae	*Pseudostaurosira brevistriata*	PSEBREV

	Pseudostaurosira parasitica	PSEPARA
	Staurosira construens	STACONS
	Staurosira construens var venter	STAVENT
Small *Navicula* spp. (*sensu lato*)	*Sellaphora nigri*	NAVMINI
	Sellaphora seminulum	SELSEMI
***Encyonopsis* spp.**	*Encyonopsis cesatii*	ENCCESA
	Encyonopsis descripta	ENCDESC
***Pinnularia* spp.**	Grouped for RDA	PINSPP
	Pinnularia gibba	<2%
	Pinnularia interrupta	<2%
	Pinnularia legumen	<2%
	Pinnularia maior/viridis	<2%
	Pinnularia microstauron	<2%
	Pinnularia nodosa	<2%
	Pinnularia obscura	<2%
	Pinnularia streptoraphe	<2%
Large *Navicula* spp.	*Navicula cryptocephala*	NAVCRC
	Navicula cryptotenella	NAVCRT
	Navicula radiosa	NAVRADI
***Brachysira* spp.**	*Brachysira styriaca*	BRASTYR
	Brachysira vitrea	BRAVITR
	Brachysira zellensis	BRAZELL
***Encyonema* spp.**	*Encyonema gracilis*	ENCGRAC
	Encyonema silesiacum	ENCSILE
	Encyonema hebridicum	<2%
	Encyonema perpusillum	<2%
***Cymbopleura* spp.**	*Cymbopleura incerta*	CYMINCE
	Cymbopleura angustata	<2%
	Cymbopleura lapponica	<2%
***Nitzschia* spp.**	*Nitzschia fonticola*	NITFONT
	Nitzschia palea	NITPAL
	Nitzschia alpina	<2%
	Nitzschia angustata	<2%
	Nitzschia intermedia	<2%
	Nitzschia recta	<2%
	Nitzschia vermicularis	<2%
Large benthic spp.	*Neidium ampliatum*	NEIAMPL
	Stauroneis phoenicenteron	STAPHOE
	Stauroneis javanica	<2%
Planktonic *Fragilaria* spp.	*Fragilaria tenera*	FRATENE
	Fragilaria nanana	<2%
	Fragilaria ulna	<2%
Centric planktonic spp.	*Discostella pseudostelligera*	CYCPSEU
	Lindavia michiganiana	CYCMICH

	Lindavia bodanica	<2%
Dominant wetland spp.	*Gomphonema acuminatum*	<2%
	Gomphonema angustatum	<2%
	Gomphonema gracile	<2%
	Gomphonema parvalum	<2%
	Gomphonema subtile	<2%
	Gomphonema truncatum	<2%
	Kobayasiella subtilissima	KOBSUBT
	Tabellaria spp	TABFLOC
	Eunotia spp. (grouped for RDA)	EUNSPP
	Eunotia bilunaris	<2%
	Eunotia circumborealis	<2%
	Eunotia formica	<2%
	Eunotia incisa	<2%
	Eunotia praerupta	<2%
	Gogorevia exilis	ACHEXIG
	Achnanthidium minutissimum	ACHMINU
	Amphora spp. (grouped for RDA)	AMPSPP
	Amphora pediculus	<2%
	Amphora thumensis	<2%
	Chamaepinnularia mediocris	CHAMEDI
	Cocconeis placentula	COCPLAC
	Delicata delicatula	DELDELI
	Denticula kuetzingii	DENKUET
	Diploneis oblongella	DIPOBLO
	Fragilaria capucina	FRACAPU
	Kobayasiella jaagii	KOBJAAG
	Microcostatus kuelbsii	MICKUEL
	Navicula leptostriata	NAVLEPT
	Navicula rhynchocephala	NAVRHYN
	Navicula vulpina	NAVVULP
	Nupela vitiosa	NUPVITI
	Sellaphora laevissima	SELLAEV
	Sellaphora pupula	SELPUPU
	Sellaphora vitabunda	SELVITA